CERN-TH.4408/86

EFFECTS OF A SUPERSTRING GAUGE BOSON ON HIGH ENERGY e^+e^- ANNIHILATION AND ep SCATTERING

V.D. Angelopoulos*), John Ellis, D.V. Nanopoulos

and

N.D. Tracas

CERN -- Geneva

ABSTRACT

We calculate the effects at LEP and HERA of the second neutral gauge boson appearing in phenomenological superstring models with an effective $SU(3)_C \times SU(2)_L \times U(1)_{Y_L} \times U(1)_{Y_R}$ gauge group. Present phenomenological constraints leave open the possibility of a measurable shift in the first Z mass, and of observable modifications to the total e^+e^- cross-section and forward-backward asymmetries at the Z peak and beyond. High energy ep scattering asymmetries may also differ significantly from the standard model predictions.

---

*) On leave of absence from Department of Theoretical Physics, Oxford University, 1 Keble Road, Oxford OX1 3NP, England.

CERN-TH.4408/86
March 1986

Compactification of the superstring[1] on a Calabi-Yau manifold[2] allows the $E_8 \times E_8'$ gauge group in the ten-dimensional theory to be broken by the Wilson loop mechanism[3] down to some subgroup $E_6 \times E_8'$ in four dimensions. The observable four-dimensional gauge subgroup of E_6 must have rank 5 or more[4], and the unique minimal rank 5 possibility $SU(3)_C \times SU(2)_L \times U(1)_{Y_L} \times U(1)_{Y_R}$ can only be realized with a very specific choice of Calabi-Yau manifold. The observable gauge subgroup is eventually broken spontaneously by the Higgs mechanism around the weak interaction scale m_W, and there could in principle be an earlier stage of gauge symmetry breaking at some scale intermediate between m_W and the original E_6 breaking scale m_X. However, the existence of an intermediate gauge symmetry breaking scale cannot be reconciled with a "no-scale" scenario for the dynamical generation of the weak interaction scale[5], and has cosmological problems[6]. Moreover, it is not possible to break a rank 6 subgroup of E_6 all the way down to $SU(3)_C \times U(1)_{em}$ at the weak interaction scale alone[5]. This leaves us with the unique minimal possibility that $E_6 \to SU(3)_C \times SU(2) \times U(1)_{Y_L} \times U(1)_{Y_R}$ at m_X, and that $SU(2)_L \times U(1)_{Y_L} \times U(1)_{Y_R} \to U(1)_{em}$ at m_W. No-scale dynamical models realizing this possibility have been constructed[7),5]. In this case, one expects just one extra neutral gauge boson Z_E with mass O(100 GeV to 1 TeV), in addition to the conventional Z^0. The couplings of this new neutral gauge boson are completely fixed, and its effects in low energy νN[7], νe[8] scattering and e^+e^-[7] annihilation, on primordial cosmological nucleosynthesis[8] and on the observed Z^0 mass[5], have been studied previously. In this paper we study the effects of the new neutral gauge boson on high energy e^+e^- annihilation, e.g., at LEP or the SLC, and in high energy ep scattering, e.g., at HERA.

In general, the new neutral gauge boson Z_E mixes[5] with the conventional Z^0, shifting its mass lower than it would have been in the standard model with the same value of $\sin^2\theta_W$. We call the two eigenstates of the (Z^0, Z_E) squared mass matrix Z and Z'. It is possible that $\sin^2\theta_W$ can be so well determined by other electroweak measurements, such as low energy neutral currents or m_W, that a significant discrepancy will be found between the value of m_{Z^0} predicted in the standard model and the observed value m_Z. At the moment, the absence of such a discrepancy is the most stringent constraint on the parameters of models[5] with this new neutral gauge boson, which are the vacuum expectation values of the three Higgs fields breaking $SU(2)_L \times U(1)_{Y_L} \times U(1)_{Y_R}$ to $U(1)_{em}$. It is also possible that these electroweak measurements will not be sufficiently precise that such a discrepancy can be established in the foreseeable future. In this case one must look for consistency between the standard model and the different measurements made at high energy e^+e^- and ep accelerators. A natural strategy is to "measure" $\sin^2\theta_W^{eff}$ by first measuring m_Z and using the standard model formula $m_Z = 38.65\ \mathrm{GeV}/\sin\theta_W^{eff}\cos\theta_W^{eff}$. In principle, mixing with the extra gauge boson would mean that $\sin^2\theta_W^{eff} \neq \sin^2\theta_W \equiv (38.65/m_W)^2$. This means that other observables, such as the total cross-section σ or the forward-backward asymmetry A on or above the Z peak in e^+e^- annihilation[9], or parity and charge asymmetries in ep collisions[10], could have observable differences from the values predicted using the standard model with $\sin^2\theta_W^{eff}$ taken from the observed Z mass.

In this paper we first recapitulate[5] the effects of mixing on the Z^0, and assess present and possible future bounds on the model parameters from measurements of the Z mass[5],[7],[8]. Next we present cross-section formulae for $e^+e^- \to \gamma^*, Z^{0*}, Z_E^* \to f\bar{f}$, where f is any fermion. Then we discuss numerically the possible differences in cross-sections and in forward-backward asymmetry measurements at and above the resonance peak, between our two-boson model and the standard model with m_{Z^0} fixed to be the same as the lighter mass eigenstate in the neutral boson mass matrix. We find that these measurements could reveal discrepancies with the standard model, even though none have become apparent in electroweak measurements to date. Finally, we also make a similar analysis for high energy ep scattering, finding that, although significant effects are possible, this is a less sensitive probe of the second neutral boson than precision measurements at the first Z peak in e^+e^- annihilation would be.

The $(\text{mass})^2$ matrix mixing the two neutral gauge bosons in our minimal superstring-inspired model is[5]

$$\begin{pmatrix} Z^0 & Z_E \end{pmatrix} m_{Z^0}^2 \begin{pmatrix} 1 & \alpha \\ \alpha & b \end{pmatrix} \begin{pmatrix} Z^0 \\ Z_E \end{pmatrix} \tag{1}$$

where $m_{Z^0} = (1/\sqrt{2})(\sqrt{g^2+g'^2})(\sqrt{v^2+\bar{v}^2})$ is the Z^0 mass in the standard model with Higgs doublets H and $\bar{H}$ of hypercharge $Y = \pm\frac{1}{2}$ with vacuum expectation values (vevs) v and $\bar{v}$ respectively, and

$$\alpha = \frac{1}{3}\sin\theta_W \frac{4v^2-\bar{v}^2}{v^2+\bar{v}^2} \tag{2a}$$

$$b = \frac{1}{9}\sin^2\theta_W \frac{25x^2+16v^2+\bar{v}^2}{v^2+\bar{v}^2} \tag{2b}$$

where x is the vev of the $SU(3)_C \times SU(2)_L \times U(1)_Y$ singlet field N. The matrix (1) gives two mass eigenstates Z and Z' with mass

$$m_{Z,Z'} = m_{Z^0}\sqrt{\frac{1}{2}\left[(1+b)\mp\sqrt{(1-b)^2+4a^2}\right]} \qquad (3)$$

Clearly $m_Z \to m_{Z^0}$ and $m_{Z'} \to \infty$ as $x/v \to \infty$ for fixed $\bar{v}/v$, and the best lower limit on x/v and hence $m_{Z'}$ comes from the agreement of the observed neutral gauge boson mass m_Z with the value of m_{Z^0} predicted in the standard model. This agreement can be quantified by comparing

$$\sin^2\theta_W \equiv \left(\frac{38.65}{m_W}\right)^2 \qquad (4a)$$

and

$$\sin^2\bar{\theta}_W \equiv 1 - m_W^2/m_Z^2 \qquad (4b)$$

We find[5)]

$$\Delta \equiv \sin^2\theta_W - \sin^2\bar{\theta}_W = 0.012 \pm 0.023 \qquad (5)$$

Taking the 1-σ limit $\Delta < 0.035$, we find[5)] the bounds on x/v and $m_{Z'}$ for different values of $\bar{v}/v$ which are shown as a dashed line in Fig. 1. Representative examples of these results are

$$\frac{x}{v} > \begin{cases} 3.2 \\ 3.8 \end{cases}, \quad m_{Z'} > \begin{cases} 210 \\ 280 \end{cases} \mathrm{GeV} \ \text{for}\ \frac{\bar{v}}{v} = \begin{cases} 0.6 \\ 0.2 \end{cases} \qquad (6)$$

where we have quoted the bounds for values of $\bar{v}/v$ in the range favoured by our previous dynamical calculations[5),*)]. In this paper, we investigate whether future measurements in high energy e^+e^- (SLC,LEP[9)]) and ep (HERA[10)]) experiments can probe beyond the bounds (6).

The obvious place to start is the Z peak, and we want to discover whether it is the Z^0 of the standard model or the Z of our two-boson model. The most accurately measured weak interaction parameter will presumably be the mass of the observed Z, and we expect prior low energy neutral current measurements to be

---

*) We do not use here the more model-dependent limits which come from primordial nucleosynthesis[8)].

consistent with the standard model with $\sin^2\theta_W$ defined by

$$\sin^2\Theta_W^{eff}: \qquad m_Z = \frac{38.65\ \mathrm{GeV}}{\sin\Theta_W^{eff}\cdot\cos\Theta_W^{eff}} \tag{7}$$

We will then compare the high energy predictions of our extended $SU(2)_L \times U(1)_{Y_L} \times U(1)_{Y_R}$ model to those of the standard model with neutral currents given by (7), with $\sin^2\theta_W \equiv (38.65\mathrm{GeV}/m_W)^2 = g'^2/g_2^2+g'^2$ adjusted so that $m_{Z^0} = m_Z$ *). We will make comparisons in the cross-sections and forward-backward asymmetries on the Z peak and at high energies ($\sqrt{s}$ = 180 GeV) in e^+e^- annihilation, and in the different charge and parity asymmetries in ep collisions ($e^-_{L,R}p - e^+_{L,R}p$, $e^\pm_L p - e^\pm_R p$).

The general form of the differential cross-section for $e^+e^- \to f\bar{f}$ via the photon and two other massive neutral gauge bosons is:

$$\frac{d\sigma}{d\cos\Theta} = \frac{2\pi}{4\cdot 64\cdot\pi^2\cdot s}\cdot\Big[4e^4Q_f^2(1+\cos^2\Theta) +$$

$$\frac{s^2}{(s-M_Z^2)^2+\Gamma^2M_Z^2}\cdot(g_{e_L}^2+g_{e_R}^2)(g_{f_L}^2+g_{f_R}^2)(1+\cos^2\Theta) +$$

$$\frac{s^2}{(s-M_{Z'}^2)^2+\Gamma^2M_{Z'}^2}\cdot(g'^2_{e_L}+g'^2_{e_R})(g'^2_{f_L}+g'^2_{f_R})(1+\cos^2\Theta) +$$

$$2\cdot\frac{(s-M_Z^2)\,e^2Q_f\,s^2}{s((s-M_Z^2)^2+\Gamma^2M_Z^2)}\cdot$$

$$\begin{Bmatrix}(g_{e_L}+g_{e_R})(g_{f_L}+g_{f_R})(1+\cos^2\Theta) - \\ (g_{e_L}-g_{e_R})(g_{f_L}-g_{f_R})\,2\cos\Theta\end{Bmatrix} + \tag{8}$$

$$2\cdot\frac{(s-M_{Z'}^2)\,e^2Q_f\,s^2}{s((s-M_{Z'}^2)^2+\Gamma^2M_{Z'}^2)}\cdot$$

$$\begin{Bmatrix}(g'_{e_L}+g'_{e_R})(g'_{f_L}+g'_{f_R})(1+\cos^2\Theta) - \\ (g'_{e_L}-g'_{e_R})(g'_{f_L}-g'_{f_R})\,2\cos\Theta\end{Bmatrix} +$$

---

*) This procedure only makes sense (i.e., gives $\sin^2\theta_W > 0$) if $x/v > 2$.

$$2\cdot\frac{\left((s-M_Z^2)(s-M_{Z'}^2)-\Gamma^2 M_Z M_{Z'}\right)}{\left((s-M_Z^2)^2+\Gamma^2M_Z^2\right)\left((s-M_{Z'}^2)^2+\Gamma^2M_{Z'}^2\right)}\cdot s^2\cdot$$

$$\left\{\begin{matrix}(g_{e_L}g'_{e_L}+g_{e_R}g'_{e_R})\cdot(g_{f_L}g'_{f_L}+g_{f_R}g'_{f_R})\,(1+\cos^2\theta)- \\ (g_{e_L}g'_{e_L}-g_{e_R}g'_{e_R})(g_{f_L}g'_{f_L}-g_{f_R}g'_{f_R})\;2\cos\theta\end{matrix}\right]\Bigg] \qquad (8)\ \text{cont.}$$

In our minimal superstring-inspired model[5)] the couplings of the physical neutral gauge bosons Z and Z' to any fermion f are combinations of those of the unmixed Z^0 and Z_E:

$$\begin{aligned} g_{f_{L,R}} &= \cos\Theta_N\, g^{Z_0}_{f_{L,R}} + \sin\Theta_N\, g^{Z_E}_{f_{L,R}} \\ g'_{f_{L,R}} &= -\sin\Theta_N\, g^{Z_0}_{f_{L,R}} + \cos\Theta_N\, g^{Z_E}_{f_{L,R}} \end{aligned} \qquad (9)$$

where the neutral boson mixing angle θ_N is given by

$$\tan 2\Theta_N = \frac{2a}{1-b} \qquad (10)$$

and the Z^0 and Z_E couplings to familiar fermions are listed in the Table. The general formula (8) can be used to compute total cross-sections $\sigma_f = \int_{-1}^{1} d(\cos\theta)d\sigma(e^+e^- \to f\bar{f})/d\cos\theta$ and forward-backward asymmetries

$$A_f \equiv \frac{\int_0^{+1} d(\cos\Theta)\frac{d\sigma(e^+e^-\to f\bar{f})}{d\cos\Theta} - \int_{-1}^{0} d(\cos\Theta)\frac{d\sigma(e^+e^-\to f\bar{f})}{d\cos\Theta}}{\int_0^{+1} d(\cos\Theta)\frac{d\sigma(e^+e^-\to f\bar{f})}{d\cos\Theta} + \int_{-1}^{0} d(\cos\Theta)\frac{d\sigma(e^+e^-\to f\bar{f})}{d\cos\Theta}} \qquad (11)$$

We will concentrate on σ_μ and A_μ since these are likely to be the most precisely measured.

Figure 2a shows the percentage changes in the total $e^+e^- \to \mu^+\mu^-$ cross-section at the Z peak, as we go from the standard model with $\sin^2\theta_W^{eff}$ to the two-boson model with the same value of m_Z *). We see that the changes in σ are quite significant, much larger than the purely statistical errors in measuring $\sigma(e^+e^- \to \mu^+\mu^-)$. [Recall that one can expect $O(10^5)$ $Z \to \mu^+\mu^-$ events in a LEP experiment, and not a small fraction of this number at the SLC if it functions as hoped.] The largest errors in measuring $\sigma(e^+e^- \to \mu^+\mu^-)$ are likely to be systematic ones arising from uncertainties in the total luminosity, but these can surely be reduced to such a level that a measurement of $\sigma(e^+e^- \to \mu^+\mu^-)$ at the Z peak becomes a very sensitive probe of the two-boson model. Figure 2b shows the corresponding percentage change in $\sigma(e^+e^- \to \mu^+\mu^-)$ at $\sqrt{s}$ = 180 GeV, chosen to be representative of LEP II energies. The effects here are not very large, and the relatively low statistics available at high energies may not enable a very sensitive test of the two-boson model to be made. However, observable effects are possible if $\Delta(S)$ is close to its present experimental limit, and the Z' mass is low.

Figure 3a shows the change in the forward-backward asymmetry A_μ(11) on the Z peak as we go from the standard model with $\sin^2\theta_W^{eff}$ to the superstring model with the same value of m_Z. The effect is large enough to be observed for a large range of values of x/v and $\bar{v}$/v which are compatible with the present constraint (5). The statistical error in A_μ is likely to be a few $\times 10^{-3}$, and the systematic errors in measuring $\sigma(e^+e^- \to \mu^+\mu^-)$ largely cancel[9]. Figure 3b shows the change in the forward-backward asymmetry A_μ at $\sqrt{s}$ = 180 GeV. We see that the effect is very small, largely because of an accidental zero in the change in A_μ, which traverses unkindly the interesting domain of our parameter space. This measurement at high energies will have very little sensitivity to our two-boson model, though it may be useful for testing other models which do not have the accidental zero appearing in Fig. 3b.

We turn now to high energy ep scattering. The differential cross-section $d^2\sigma/dxdy$, including γ, Z and Z' exchange is:

$$\frac{d^2\sigma}{dxdy} = \frac{d^2\sigma^\gamma}{dxdy} \cdot \sum_{i,j} G_n^i G_n^j P^i P^j \left(A^{ij}(x) + \xi_n B^{ij}(x) f(y)\right) \qquad (12)$$

---

*) We have fixed Γ_Z = 2.8 GeV, as expected in the standard model, in making this comparison. We have checked that in interesting ranges of the parameters x/v and $\bar{v}$/v the width Γ_Z in the two-boson model differs from that in the standard mode by less than 1%.

where the G_n^i are the couplings of the i^{th} neutral boson to the incoming lepton: the photon corresponds to i = 1 so that $G_n^1 = -1$ for e_L^-, e_R^-, e_L^+, e_R^+, while the correspondence of G_n^2 and G_n^3 with the g's of Eqs. (9) is

$$G^2_{L,R} = (2/g_2)\cdot g_{L,R} \quad \text{and} \quad G^3_{L,R} = (2/g_2)\cdot g'_{L,R}$$

The P^i are the propagators (conveniently normalized) for the vector bosons i:

$$P^1 = 1 \qquad \text{and} \qquad P^i = \frac{Q^2}{8\sin^2\theta_W\,(M^2_{Z_i}+Q^2)} \text{ for } i>1 \tag{13}$$

where Q^2 is the transferred momentum squared. In Eq. (12), $A^{ij}(x)$ and $B^{ij}(x)$ are products of couplings of the i and j bosons to the quarks and are given by:

$$A^{ij}(x) = \frac{1}{2}\,\frac{\sum_q \left(G^i_{q_L} G^j_{q_L} + G^i_{q_R} G^j_{q_R}\right)\left(q(x)+\bar{q}(x)\right)}{\sum_q e_q^2\left(q(x)+\bar{q}(x)\right)}$$

(14)

$$B^{ij}(x) = \frac{1}{2}\,\frac{\sum_q \left(G^i_{q_L} G^j_{q_L} - G^i_{q_R} G^j_{q_R}\right)\left(q(x)+\bar{q}(x)\right)}{\sum_q e_q^2\left(q(x)+\bar{q}(x)\right)}$$

where e_q is the charge of the quark q, q(x) and $\bar{q}(x)$ are the distribution functions of the quarks and antiquarks in the proton and the $G^i_{q_{L,R}}$ are the couplings of the quarks to the boson i. The correspondence with the g's of Eq. (9) is as before, e.g., the coupling with the first Z, i = 2:

$$G^2_{q_{L,R}} = (2/g_2)(g^q_{L,R}) \text{ where } q = u, d, s, \ldots .$$

Finally, in Eq. (12)

$$f(y) = \frac{(y - y^2/2)}{(1 - y + y^2/2)} \tag{15a}$$

and

$$\xi_n = \begin{cases} +1 & \text{for } n = e_L^-, e_L^+ \\ -1 & \text{for } n = e_R^-, e_R^+ \end{cases} \tag{15b}$$

Moreover, we have used the usual variables for deep inelastic scattering defined by:

$$x \equiv \frac{Q^2}{2m_p\nu} \quad , \quad y \equiv \frac{\nu}{\nu_{max}} \quad , \quad \nu_{max} \equiv \frac{2E_eE_P}{m_p}$$

$$\text{and} \quad \nu \equiv \frac{p\cdot q}{m_p} \quad \text{with} \quad q^2 = -Q^2 \tag{16}$$

where (E_p, P) are the energy and momentum of the proton and E_e the energy of the electron. Although it may be possible to beat the systematic errors in measuring $d^2\sigma/dxdy$ down sufficiently to test the two-boson model sensitively, we have chosen to focus on the asymmetries which are usually touted as sensitive tests of the standard model[11]. These are the parity asymmetries

$$A^{\pm} \equiv \frac{\frac{d^2\sigma(e_L^{\pm})}{dxdy} - \frac{d^2\sigma(e_R^{\pm})}{dxdy}}{\frac{d^2\sigma(e_L^{\pm})}{dxdy} + \frac{d^2\sigma(e_R^{\pm})}{dxdy}} \tag{17a}$$

and the charge asymmetries

$$A^c_{L,R} \equiv \frac{\frac{d^2\sigma(e^-_{L,R})}{dxdy} - \frac{d^2\sigma(e^+_{L,R})}{dxdy}}{\frac{d^2\sigma(e^-_{L,R})}{dxdy} + \frac{d^2\sigma(e^+_{L,R})}{dxdy}} \tag{17b}$$

We have plotted the changes δA in these quantities as functions of x/v and $\bar{v}/v$ in Fig. 4, choosing the following values of the kinematic variables: $\sqrt{s}$ = 314 GeV corresponding to the HERA design, x = 0.25 and y = 0.5 and using the quark and antiquark distributions of Ref. 12). Undoubtedly the most sensitive test of the two-boson model would involve a global fit of data at all values of x and y, but the results in Fig. 4 should be representative. Figure 4a shows the change in the parity asymmetry in A_p^- (17a), which is 0.17 in the standard model for these values of the kinematic variables. We see that the present bound on $\Delta(S)$ still allows changes in A_p^- of several per cent. Figure 4b shows the corresponding changes in A_p^+ (-0.16 in the standard model), which is considerably smaller. Figure 4c shows the change in the charge asymmetry A_L^C (0.35 in the standard model), which is also very small in the domain of interest. Finally, Fig. 4d shows the change in A_R^C (0.03 in the standard model) which is large compared to A_R^C itself, but small in overall magnitude.

Comparing Figs. 2, 3 and 4 we see that while all show some observable deviations from the standard model, the most sensitive measurements will presumably be those of $\sigma(e^+e^- \rightarrow \mu^+\mu^-)$ and A_μ on the Z peak, in part because of the larger statistics to be expected there. As one would hope, measurements at high energies in e^+e^- and ep collisions can probe the parameters of our two-boson model inspired by the superstring, beyond the limits established by present measurements of neutral current parameters and of the Z mass in particular.

ACKNOWLEDGEMENTS

We thank D. Loucas for help with the graphs. One of us (V.D.A.) thanks the Ministry of National Economy of Greece for financial support.

Table

Vector and axial couplings to Z^0 and Z_E

	$u(= c = t)$	$d(= s = b)$	$e(= \mu = \tau)$	$\nu_e(= \nu_\mu = \nu_\tau)$
$g_L^{Z^0}$	$\frac{\frac{1}{2} - \frac{2}{3}\sin^2\theta_W}{\cos\theta_W} g_2$	$\frac{-\frac{1}{2} + \frac{1}{3}\sin^2\theta_W}{\cos\theta_W} g_2$	$\frac{-\frac{1}{2} + \sin^2\theta_W}{\cos\theta_W} g_2$	$\frac{\frac{1}{2}}{\cos\theta_W} g_2$
$g_R^{Z^0}$	$\frac{-\frac{2}{3}\sin^2\theta_W}{\cos\theta_W} g_2$	$\frac{\frac{1}{3}\sin^2\theta_W}{\cos\theta_W} g_2$	$\frac{\sin^2\theta_W}{\cos\theta_W} g_2$	0
$g_L^{Z_E}$	$\sqrt{\frac{3}{5}}\,(\frac{1}{3})\, g_E$	$\sqrt{\frac{3}{5}}\,(\frac{1}{3})\, g_E$	$\sqrt{\frac{3}{5}}\,(-\frac{1}{6})\, g_E$	$\sqrt{\frac{3}{5}}\,(-\frac{1}{6})\, g_E$
$g_R^{Z_E}$	$\sqrt{\frac{3}{5}}\,(-\frac{1}{3})\, g_E$	$\sqrt{\frac{3}{5}}\,(\frac{1}{6})\, g_E$	$\sqrt{\frac{3}{5}}\,(-\frac{1}{3})\, g_E$	$\sqrt{\frac{3}{5}}\,(-\frac{5}{6})\, g_E$

REFERENCES

1) J.H. Schwarz, Physics Reports 89C (1982) 223;
M.B. Green, Surv. High Energy Phys. 3 (1983) 127.

2) P. Candelas, G.T. Horowitz, A.Strominger and E.Witten, Nucl. Phys.B258 (1985) 46.

3) Y. Hosotani, Phys. Lett. 126B (1983) 309.

4) E. Witten, Nucl. Phys. B258 (1985) 75;
M. Dine, V. Kaplunovsky, M. Mangano, C. Nappi and N. Seiberg, Nucl. Phys. B259 (1985) 519.

5) J. Ellis, K. Enqvist, D.V. Nanopoulos and F. Zwirner, CERN preprints TH.4323/85 (1985) and TH.4350/86 (1986).

6) K. Enqvist, D.V. Nanopoulos and M. Quiros, CERN preprint TH.4335/85 (1985).

7) E. Cohen, J. Ellis, K. Enqvist and D.V. Nanopoulos, Phys. Lett. 165B (1985) 76

8) J. Ellis, K. Enqvist, D.V. Nanopoulos and S. Sarkar, Phys. Lett 167B (1986) 457.

9) "Physics at LEP", eds. J. Ellis and R. Peccei, CERN Report 86-02 (1986).

10) R. Cashmore et al., Physics Reports 122C (1985)275.

11) A. Love, D.V. Nanopoulos and G.G. Ross, Nucl. Phys. B49 (1972) 513.

12) M. Clück, E. Hoffmann and E. Reya, Z. Phys. C13 (1982) 119.

FIGURE CAPTIONS

Fig. 1 : Contours of $\Delta(S)$ and of m_Z, in the $(x/v, \bar{v}/v)$ plane. The present 1-σ bound $\Delta < 0.035$ is indicated by a dashed line. In this and subsequent figures we use $\sin^2\theta_W^{eff} = 0.22$, but the results are not very sensitive to this assumed value.

Fig. 2 : Percentage changes in $\sigma(e^+e^- \to \mu^+\mu^-)$ from the standard model to the superstring-inspired model with the same value of m_Z: (a) for $\sqrt{s} = m_Z$, (b) for $\sqrt{s}$ = 180 GeV. The dashed line corresponds to $\Delta = 0.035$.

Fig. 3 : Changes in the forward-backward asymmetry A_μ (11) from the standard model to the superstring-inspired model with the same value of m_Z: (a) for $\sqrt{s} = m_Z$, (b) for $\sqrt{s}$ = 180 GeV. The dashed line corresponds to $\Delta = 0.035$.

Fig. 4 : Changes in the parity asymmetries (a) A_p^- and (b) A_p^+, and in the charge asymmetries (c) A_L^C and (d) A_R^C. All are calculated for $\sqrt{s}$ = 314 GeV, $x = 0.25$ and $y = 0.5$. The dashed line corresponds to $\Delta = 0.035$.

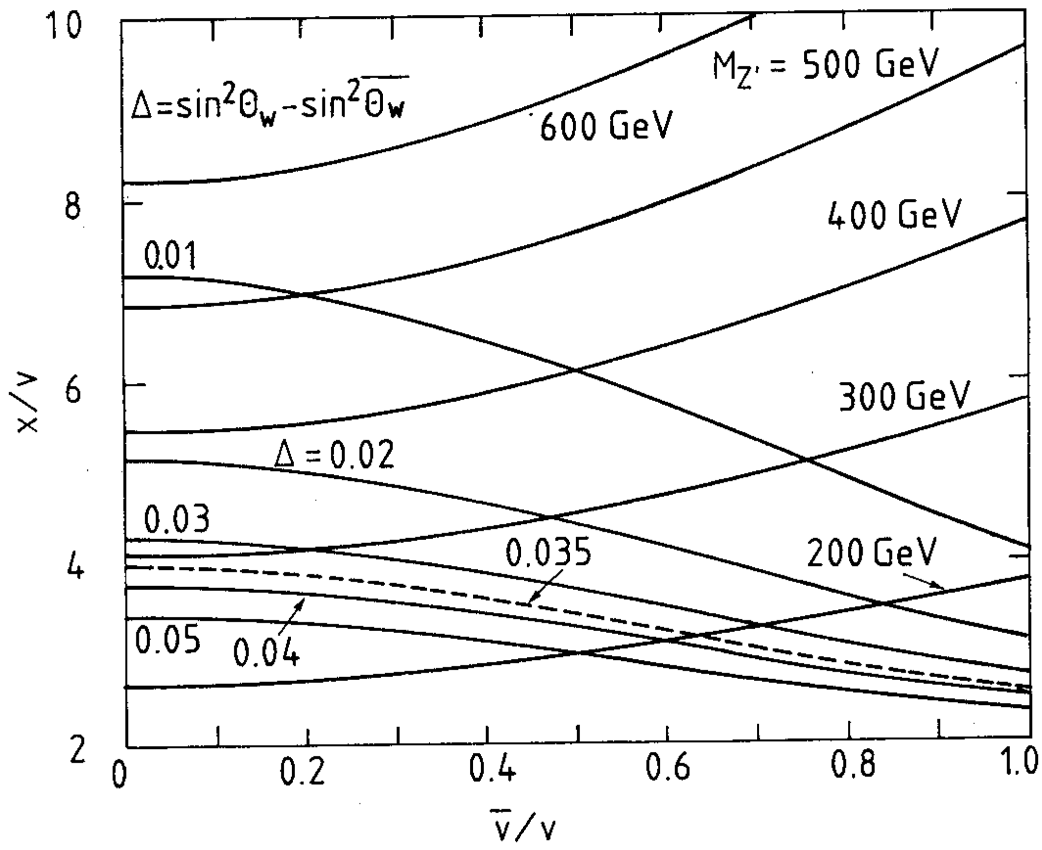

10
8
6
4
2
x/v
0
0.2
0.4
0.6
0.8
1.0
$\bar{v}/v$
$\Delta=\sin^2\theta_w-\sin^2\overline{\theta_w}$
$M_{Z'}$ = 500 GeV
600 GeV
400 GeV
300 GeV
200 GeV
0.01
Δ = 0.02
0.03
0.035
0.05
0.04

Fig. 1

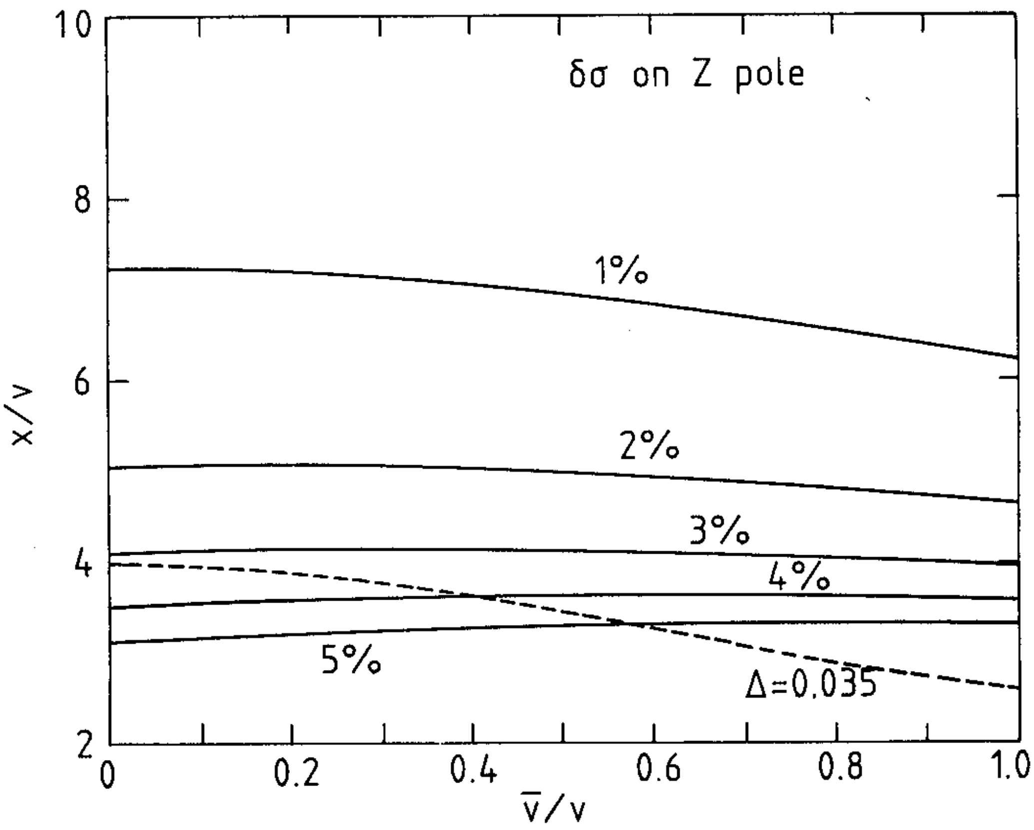

Fig. 2a

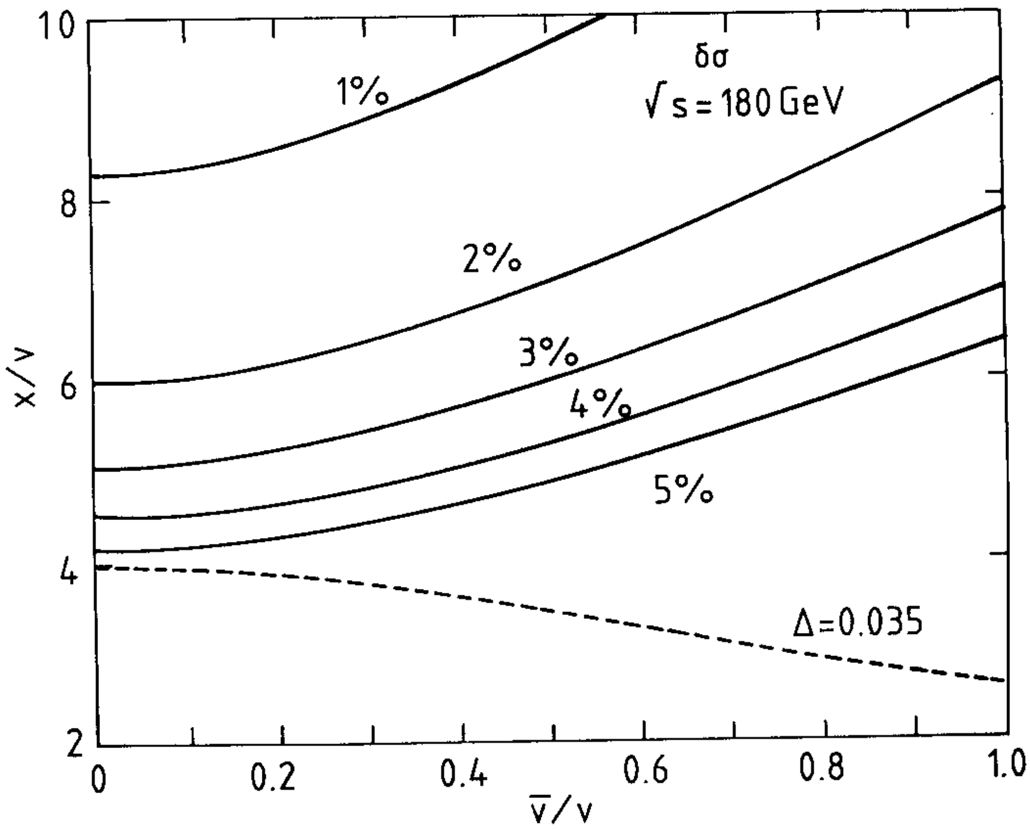

Fig. 2b

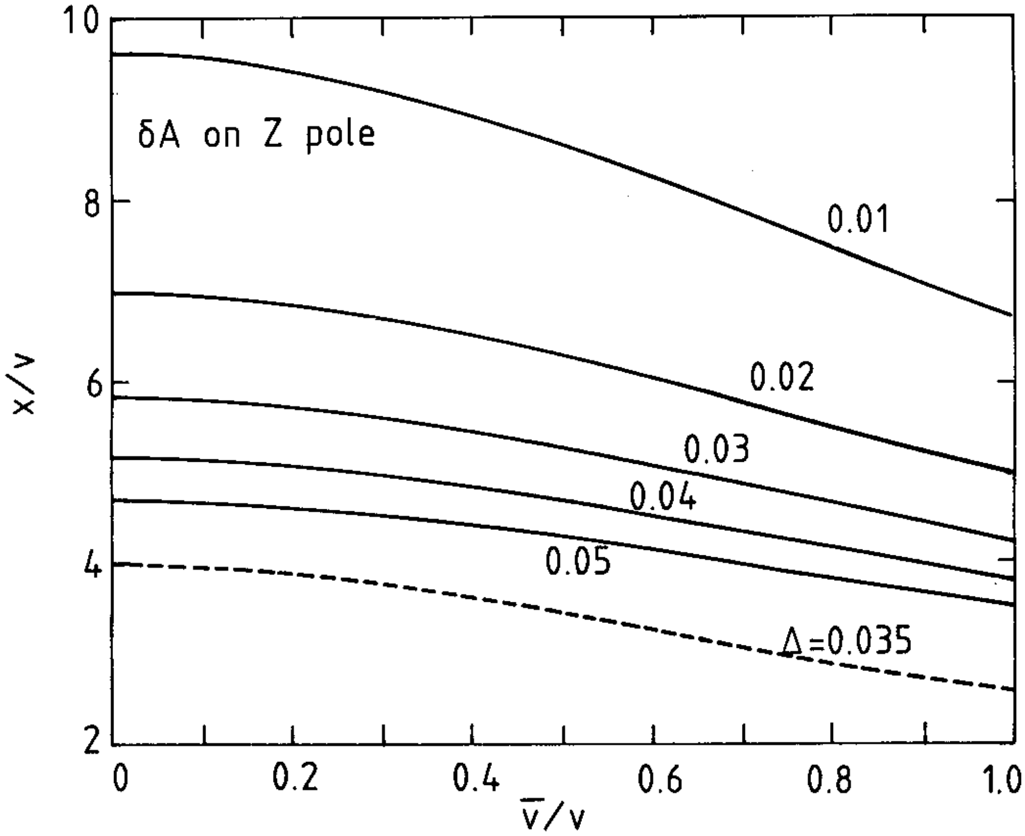

δA on Z pole
0.01
0.02
0.03
0.04
0.05
Δ=0.035
x/v
$\bar{v}$/v

Fig. 3a

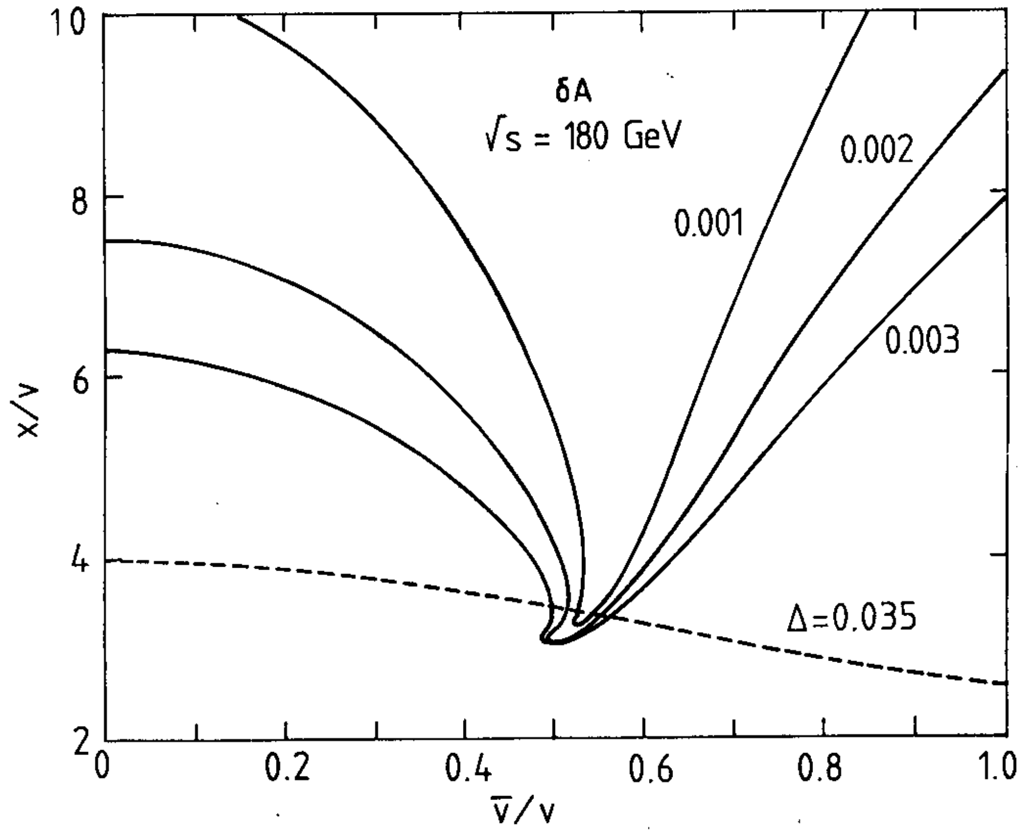

δA
√s = 180 GeV
0.001
0.002
0.003
Δ=0.035
x/v
$\bar{v}$/v

Fig. 3b

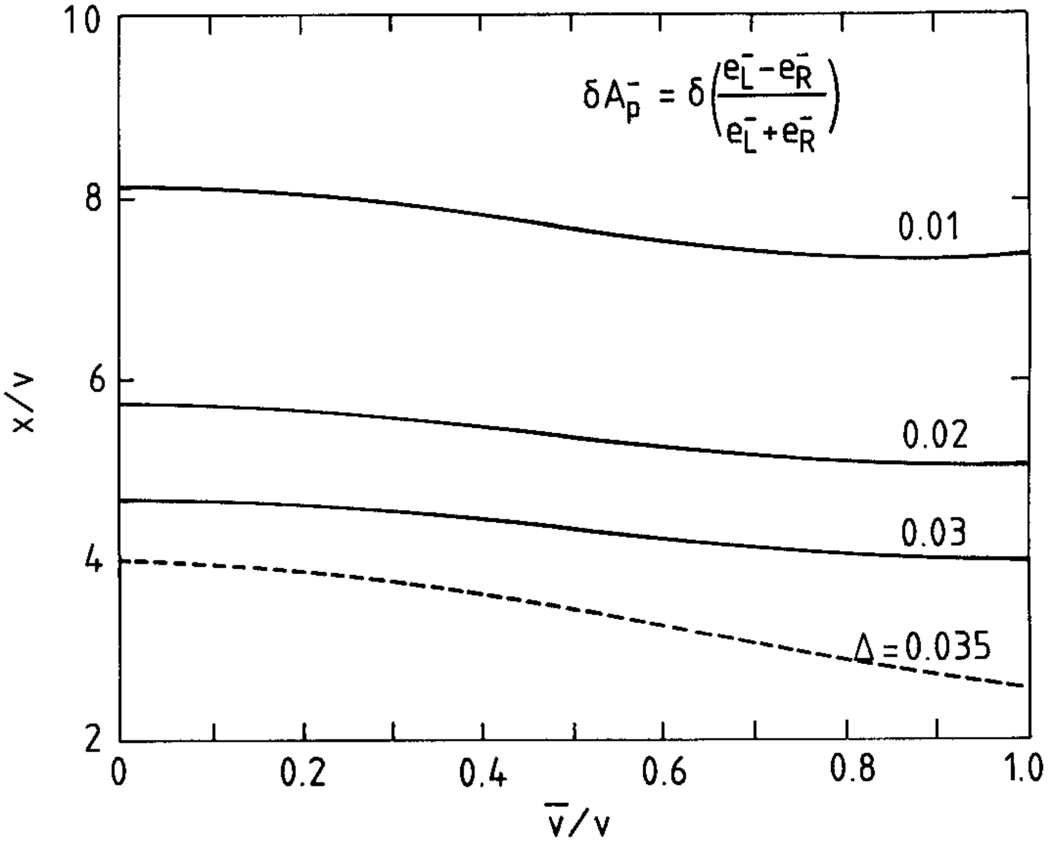

$\delta A_p^- = \delta\left(\frac{e_L^- - e_R^-}{e_L^- + e_R^-}\right)$
0.01
0.02
0.03
$\Delta = 0.035$
10
8
6
4
2
x/v
0
0.2
0.4
0.6
0.8
1.0
$\overline{v}/v$

Fig. 4a

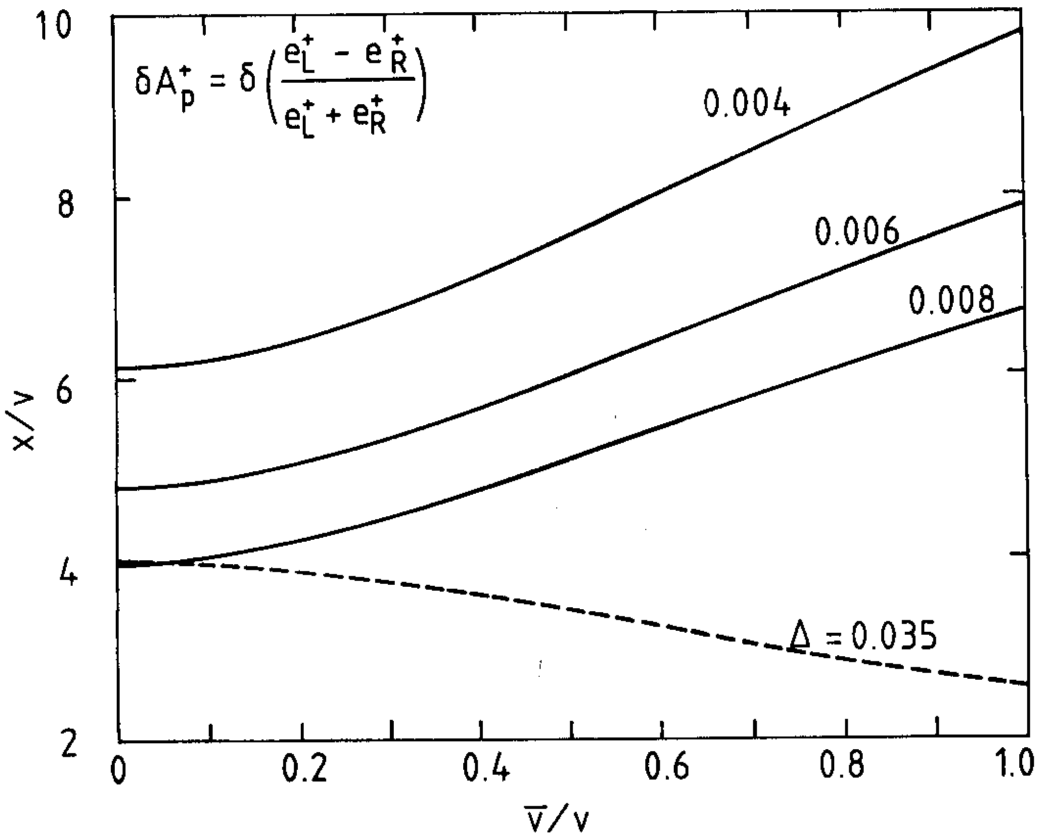

$\delta A_p^+ = \delta\left(\frac{e_L^+ - e_R^+}{e_L^+ + e_R^+}\right)$
0.004
0.006
0.008
$\Delta = 0.035$
10
8
6
4
2
x/v
0
0.2
0.4
0.6
0.8
1.0
$\overline{v}/v$

Fig. 4b

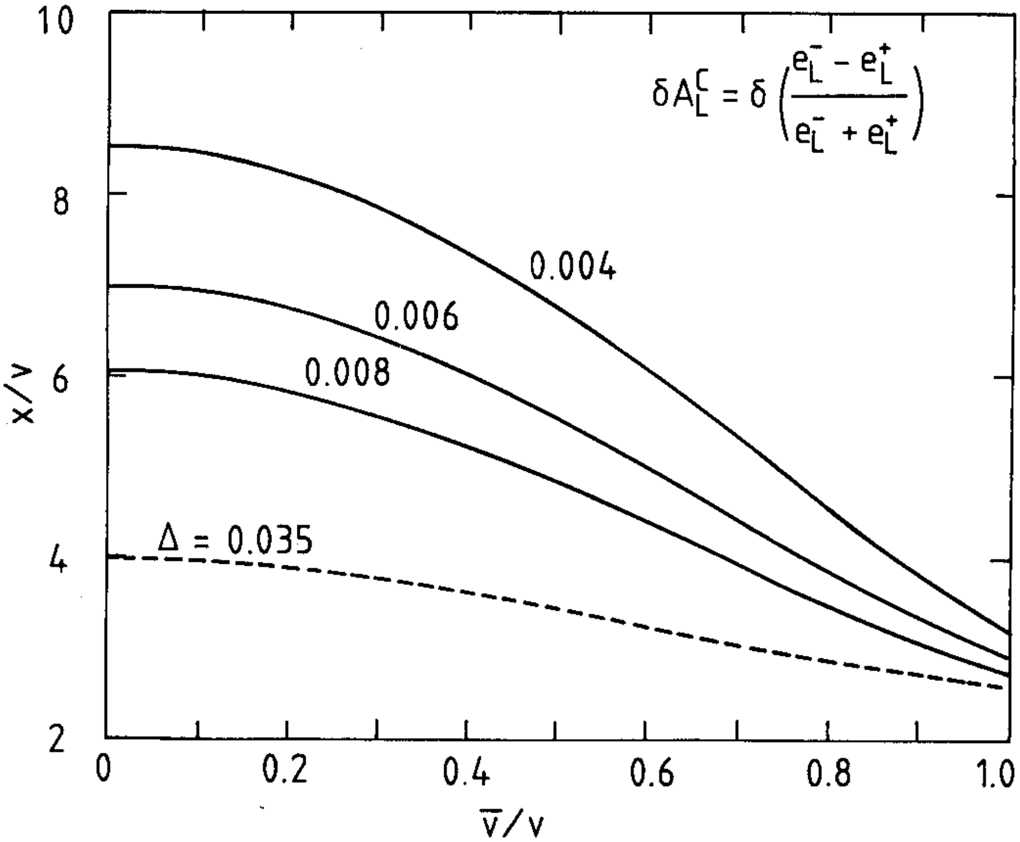

10
8
6
4
2
x/v
$\delta A_L^C = \delta\left(\frac{e_L^- - e_L^+}{e_L^- + e_L^+}\right)$
0.004
0.006
0.008
Δ = 0.035
0
0.2
0.4
0.6
0.8
1.0
$\overline{v}/v$

Fig. 4c

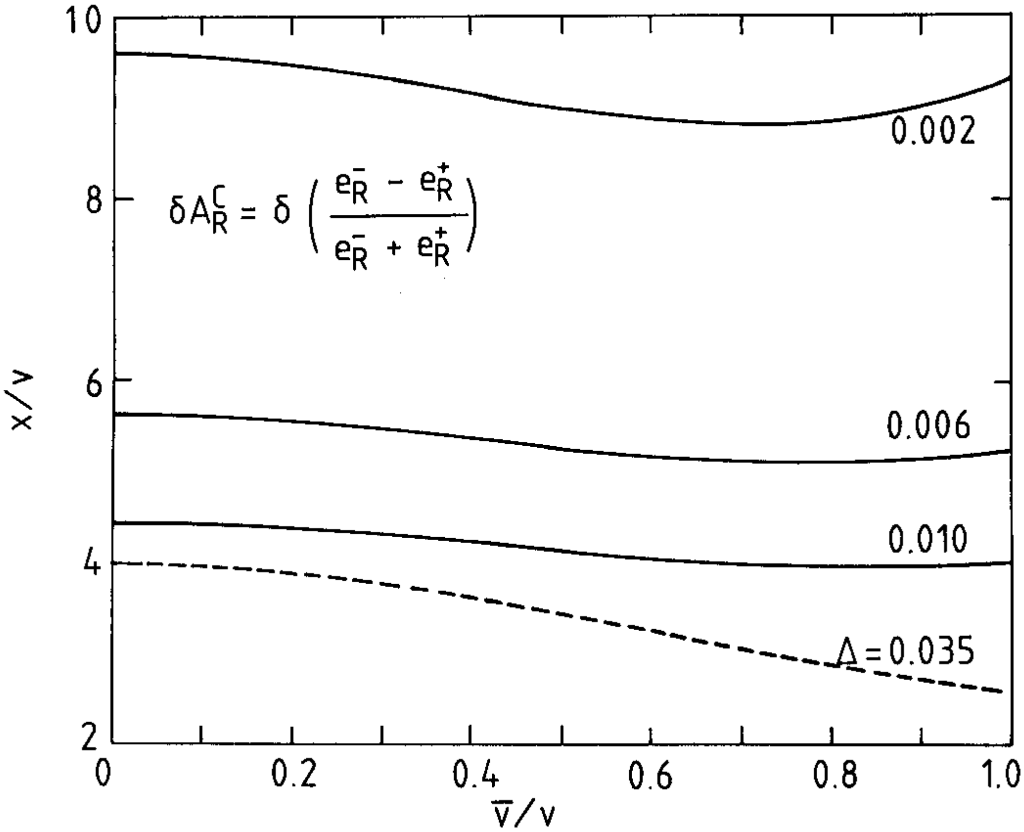

10
8
6
4
2
x/v
$\delta A_R^C = \delta\left(\frac{e_R^- - e_R^+}{e_R^- + e_R^+}\right)$
0.002
0.006
0.010
Δ=0.035
0
0.2
0.4
0.6
0.8
1.0
$\overline{v}/v$

Fig. 4d